Linear assemblies of nanoparticles electrostatically organized on DNA scaffolds

MARVIN G. WARNER AND JAMES E. HUTCHISON*

Department of Chemistry and Materials Science Institute, University of Oregon, Eugene, Oregon 97403, USA
*e-mail: hutch@oregon.uoregon.edu

Published online: 9 March 2003; doi:10.1038/nmat853

A significant challenge faced in the use of nanoscale building blocks is developing parallel methods for interconnecting and patterning assemblies of the individual components. Molecular or polymeric scaffolds hold promise as a means of preparing closely spaced, specifically arranged nanoscale assemblies. Here we show how a biopolymer, DNA, can be used as a scaffold for the assembly of extended, close-packed, ligand-stabilized metal nanoparticle structures, including several desirable architectures (such as lines, ribbons, and branches). Electrostatic binding of ligand-stabilized nanoparticles to the DNA backbone results in extended linear chain-like structures, ribbon-like structures composed of parallel nanoparticle chains, and branched structures. High-resolution transmission electron microscopy shows that the particles are evenly spaced, separated only by the 15 Å imposed by the intervening ligand shell. These studies demonstrate that biomolecular nanolithography (the arrangement of nanoscale building blocks on biomolecular scaffolds) is a viable approach to interconnecting individual devices into extended, closely spaced assemblies.

The miniaturization of the transistor has had an enormous impact on technology and fuelled many important research efforts in the materials sciences. As the transistor and other electronic devices are miniaturized to nanoscale dimensions, traditional silicon processing techniques and device architectures begin to fail. The push towards miniaturization has focused considerable attention on the use of macromolecules and small molecules as new building blocks for electronic devices[1–6]. For example, the construction of a nanoscale transistor by using carbon nanotubes has recently been reported[7,8]. Small molecules, particularly those with π-conjugated structures, have also shown potential as functional components in electronic devices[1,7,9–12]. Nanoparticles with diameters of one to a few nanometres are particularly attractive candidates, with dimensions that lie conveniently between those of larger building blocks (such as nanotubes) and small molecules. Recently both metal and semiconductor nanoparticles have been used as the functional components of nanoscale electronic devices[13–17]. The above examples show that several nanoscale building blocks can be used as individual devices.

A general challenge in nanoscience involves finding methods to organize, interconnect and address individual nanostructures on surfaces[18]. Extended linear and branched chains of closely spaced[19] nanoparticles are thus desirable target structures[13,19–21] because they could be used as nanoscale interconnects and as building blocks for active nanodevices.

Biomolecular nanolithography, the patterning of nanoscale building blocks on biopolymer scaffolds, is a versatile approach to organizing and interconnecting assemblies of nanoparticles on surfaces[13,22]. In particular, polypeptides and polynucleotides (DNA and RNA) have been widely investigated as scaffolds because of their structural diversity, well-defined polymeric sequences, and wealth of side-chain and backbone functionalities that can be used to attach nanoparticles to the scaffolding (for example, electrostatics, groove binding and intercalation)[23–25]. For applications in which the electronic properties of the assemblies are important, a unique advantage of scaffolding methods is the ability to separate structural (provided by the scaffold) and electronic (provided by the nanoparticles) properties. Few studies report examples[26–30] of such scaffolding methods; however, in those that do, assemblies with consistent interparticle spacing and long-range order are rare.

Here we demonstrate the use of DNA scaffolds to pattern closely spaced gold nanoparticle assemblies of lines, ribbons and junctions

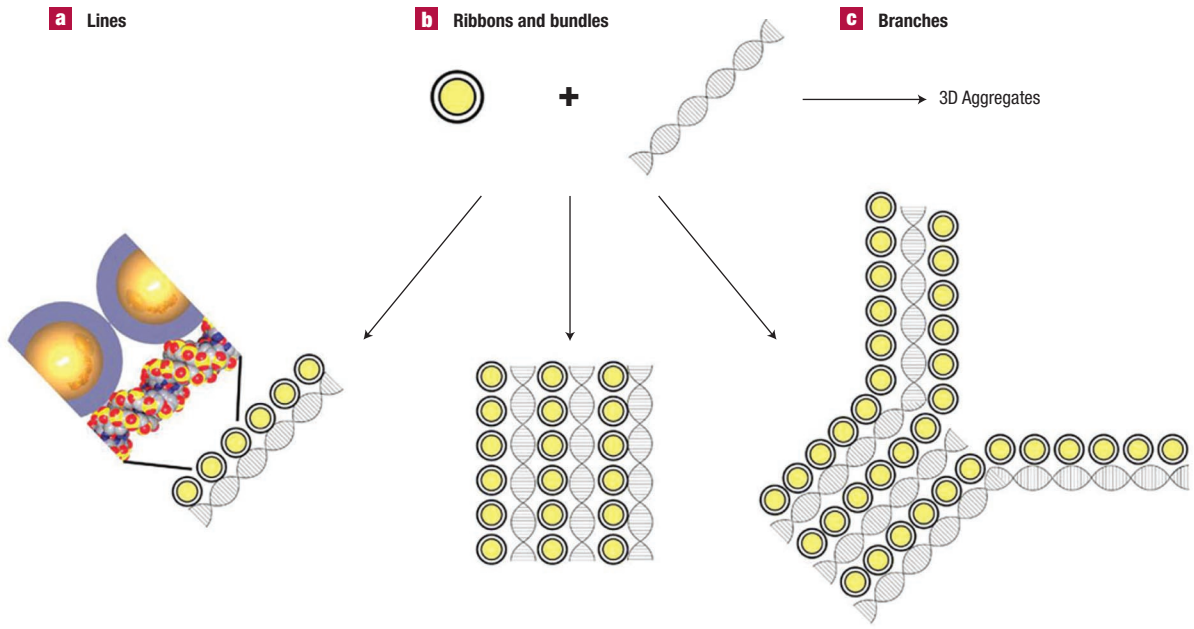

Figure 1 Nanoassemblies of gold nanoparticles formed during solution phase assembly. Electrostatic assembly of cationic nanoparticles onto the anionic backbone of DNA produces a wide range of structures including **a**, closely spaced linear arrays, **b**, ribbons or bundles comprising multiple parallel chains, and **c**, branched assemblies wherein a ribbon structure splits into narrower ribbon assemblies. Owing to the polyvalency of both building blocks (nanoparticles and DNA), three-dimensional aggregates are formed at long incubation times.

on surfaces. The nanoparticles form close-packed linear assemblies along the DNA scaffold and show extended linear structures that often reach nearly 1 μm in length. Two-dimensional, ribbon-like structures are also observed, resulting from the cross-linking of DNA scaffolds by the polyvalent gold nanoparticles. A similar degree of order observed in the linear structures is present in the ribbons. Further, these two-dimensional (2D) ribbon structures also form well-defined branched assemblies. The work presented below provides some of the first direct microscopic evidence that demonstrates the viability of biomolecular nanolithography as a technique to pattern low-dimensional extended structures on surfaces.

In the interest of developing a general method for the solution phase assembly of low-dimensional gold nanoparticle chains onto a biomolecular scaffold (DNA), we exploited the electrostatic interaction between the negatively charged phosphate backbone of DNA and a functionalized gold nanoparticle with a cationic headgroup in the ligand shell. Generation of the nanoassemblies in solution minimizes or eliminates non-specific binding of the nanoparticles to the substrate. Because accurate determination of the spacing of the nanoparticles is of primary concern for the investigation of electronic properties of the assemblies, transmission electron microscopy (TEM) was chosen to image the structures.

The nanoparticles are synthesized according to previously reported methods[18,31,32] from a triphenylphosphine passivated precursor nanoparticle by a biphasic ligand exchange reaction with thiocholine (N,N,N-trimethylaminoethanethiol iodide)[13,33]. Assembly for the TEM involves mixing the readily available λ-DNA *Hind*III—an extended double-stranded DNA (the sample is composed of seven fragments of differing lengths ranging from ~8 μm (23,130 base pairs) to ~42 nm (125 base pairs)—with the nanoparticles in an unbuffered aqueous solution and aerosoling this mixture onto a silicon-monoxide-coated TEM grid after a given incubation period. This preparation yields assemblies that demonstrate a high degree of structural order and a low degree of free nanoparticles on the substrate. The remainder of this paper will focus on the types of structures formed by using the solution-phase assembly technique, provide some explanation about the mechanism of formation of each type of assembly, and discuss reasons why the ligand-stabilized nanoparticle assemblies are observed to be close-packed and extended.

We captured representative 'snapshots' of the assembly by aerosoling samples of the reaction mixture onto TEM grids at different incubation times. Although the assembly conditions (including concentrations of the building blocks and scaffold) were designed to generate linear chain-like structures formed by decoration of DNA with nanoparticles as shown in Fig. 1a, because of the polyvalent character of both building blocks, we expected to (and did) observe higher-order 3D aggregates/assemblies as well. On analysis by TEM, we also observed two unexpected structural types, 2D ribbons (Fig. 1b) and branched assemblies (Fig. 1c), in addition to the lines and 3D assemblies. The abundance of each type of structure was found to depend on the concentrations of the two building blocks in solution and the amount of time that the solution was incubated before the TEM sample was prepared. Longer incubation times and higher building block concentrations lead to more 2D and 3D assemblies on the TEM grid.

A striking feature observed on all TEM grids analysed by using these assembly conditions is extended closely spaced linear nanoparticle chains such as shown in Fig. 2a. The assembly shown in Fig. 2a is representative of the linear structures assembled under these conditions. It displays the features commonly observed, including extended chains, closely and evenly spaced nanoparticles, and a surprising degree of linearity.

All of the linear assemblies observed by TEM display an extended chain-like structure. The length of these assemblies (up to nearly 1 μm) is not surprising because the longest of the λ-DNA fragments is nearly 8 μm. However, the degree of coverage of the DNA by the nanoparticles is surprising because of the expected electrostatic repulsion between the

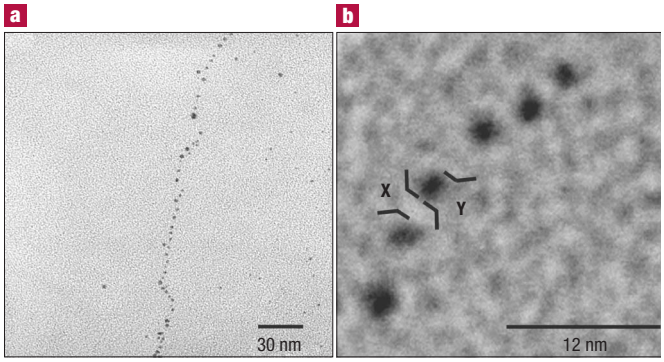

Figure 2 Transmission electron microscopy (TEM) of close-packed, linear nanoparticle/DNA assemblies. a, TEM micrograph of a nanoparticle/DNA assembly made up of a single λ-DNA scaffold. The linear assemblies are observed to have an extended structure, with some of the larger assemblies reaching nearly 1 μm in length. Over these distances the particles are observed to be closely and evenly spaced along the DNA scaffold. **b**, TEM micrograph of an expanded portion of the assembly showing that the average interparticle spacing is uniform along the DNA scaffold. The average interparticle spacing $X = 1.4 \pm 0.5$ nm ($n = 130$) consistent with a close-packed arrangement of the nanoparticles along the DNA scaffold. The average diameter of the nanoparticles $Y = 1.9 \pm 0.8$ nm ($n = 790$).

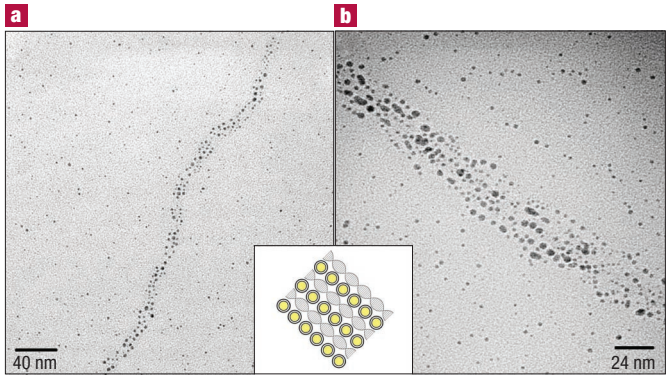

Figure 3 Ribbon-type assemblies composed of multiple λ-DNA scaffolds cross-linked by the gold nanoparticles. TEM micrographs of two sections of nanoparticle/λ-DNA ribbons that are composed of multiple λ-DNA scaffolds linked by particles on neighbouring assemblies as shown in the inset. **a**, An assembly composed of parallel λ-DNA scaffolds cross-linked by the polyvalent gold nanoparticles. **b**, A higher-order assembly composed of multiple nanoparticle/DNA assemblies.

highly charged nanoparticles. The large distances over which these assemblies extend also points to the overall robustness (see below) of the structures formed with this method. In some cases, the linear assemblies terminated at or bridged the higher-order 2D and 3D assemblies also present on the grid.

Further analysis of the linear structures confirms and quantifies the initial observations that suggested a close-packed arrangement of the ligand-stabilized particles along the DNA scaffold. Size analysis of linear nanoparticle/λ-DNA assemblies imaged by TEM gives an average interparticle spacing along the DNA scaffold of 1.4 ± 0.5 nm ($n = 130$) and an average particle size of 1.9 ± 0.8 nm ($n = 790$). Figure 2b shows a representative example of the images that were used to make these measurements. The calculated interparticle spacing for a close-packed assembly of ligand-stabilized gold nanoparticles functionalized with the thiocholine ligand would be approximately 1.3 nm (approximately twice the length of thiocholine ligand assuming no appreciable interdigitation), showing the measured value to be in good agreement with calculation. Although others have reported scaffolding studies in which nanoparticles interact with a DNA strand[26–30] these are the first extended linear assemblies in which well-separated ligand-stabilized transition metal nanoparticle cores can be clearly visualized.

The high degree of linearity observed in assemblies on single λ-DNA scaffolds such as that shown in Fig. 2 is surprising[34]. Given that the persistence length of B-form DNA has been reported to be around 53 nm[35,36], almost linear structures spanning a range of lengths up to nearly 1 μm were not expected. In addition, based upon much work on protein–DNA interactions, one might conclude that, at least for instances of low particle coverage, nanoparticle binding would cause significant DNA bending[37]. In our system, where we observe full coverage of the particles, the assemblies do not appear to bend, but adopt a linear arrangement. This could be due to the electrostatic repulsion of neighbouring particles along the chain, a structural change in the DNA[38,39], or structural reinforcement of the scaffold by the nanoparticles[40].

The large number of particles in each assembly, the close packing of those particles, and the linearity of the assemblies may provide some insight into the possible mechanism of assembly. The highly (positively) charged nanoparticles should be electrostatically attracted to the anionic DNA strand. On the other hand, one might have expected electrostatic repulsion between neighbouring particles to result in a larger spacing between the particles than we observe. If the particles bind to the DNA strand and are fixed at a specific location, then the spacing of the particles might be irregular and dominated by the electrostatic repulsion between the particles. Our observations suggest another possibility: that binding of the particles to the DNA might occur through a nucleation and growth mechanism analogous to the assembly of oligo- or poly-lysines along a DNA scaffold[41].

In poly-L-lysine (a large polycation to which our cationic nanoparticles are somewhat analogous) binding to a DNA strand is cooperative[42]. The electrostatic repulsion that could potentially prevent full coverage of the strand is overcome by an interaction that is favourable between nearest neighbours (perhaps because of a conformational change within the DNA strand on poly-L-lysine binding)[39,43]. Thus, in the lysine system, the initial binding event (nucleation) induces a structural change in the DNA that allows subsequent formation (growth) of the peptide assembly despite the possible electrostatic repulsion between closely spaced neighbours[41].

In the nanoparticle assemblies we observe, one might explain the observation of close-packed ligand-stabilized nanoparticle assemblies by an analogous nucleation and growth mechanism, and experiments are planned to test this hypothesis. An alternative mechanism by which closely spaced assemblies might be formed is through migration of particles along the scaffold after an initial binding event. The fact that charged proteins can migrate[44,45] along the DNA strand once bound offers support for the idea that the nanoparticles might display similar behaviour, allowing dispersed particles to consolidate into closely spaced assemblies along the DNA scaffold. Electrostatic repulsion between neighbouring nanoparticles might explain the extended linearity observed in the 1D assemblies. Investigation of the detailed mechanism of assembly should provide a better understanding of the formation of these assemblies, allowing the fine-tuning of the resultant structures for specific applications.

Because the nanoparticle building blocks are multivalent (possessing about 100 ligands per nanoparticle, each of which is terminated with a quaternary ammonium head group), they are capable of cross-linking the DNA scaffolds to form 2D structures. TEM images,

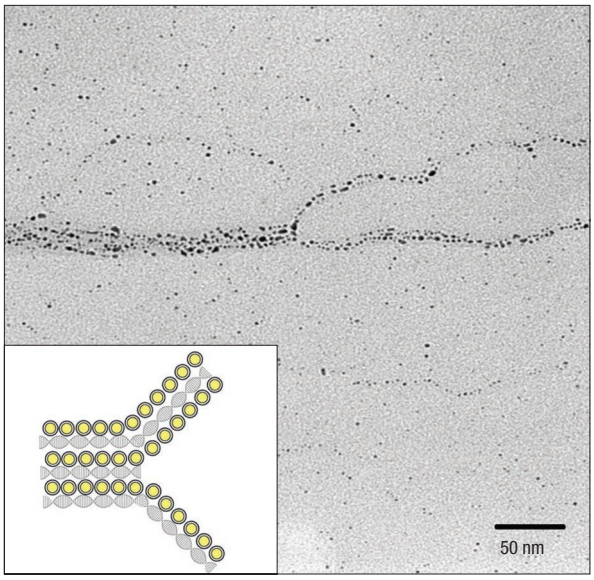

Figure 4 TEM micrograph of a branching portion of a nanoparticle/DNA assembly. TEM micrograph shows a representative example of a branched assembly. In these commonly observed features the overall dimension of the ribbon assembly is preserved in the daughter arms. The inset shows the idealized version of this type of structure where the end of a single scaffold contained within the parent ribbon assembly leads to a branch point of the remaining scaffolds.

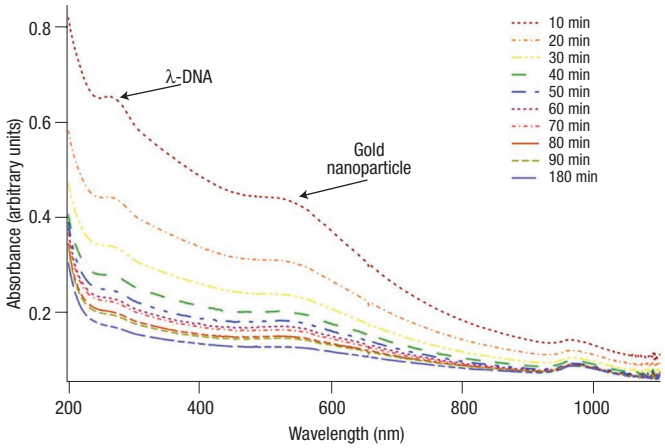

Figure 5 Monitoring the assembly process in solution by ultraviolet-visible spectroscopy. A series of ultraviolet-visible spectra collected to monitor the interaction between the functionalized gold nanoparticles and the λ-DNA. The nanoparticles and λ-DNA cross-link to form a dark precipitate which accounts for the decrease in the absorbances of the two species. Spectra were collected every 10 min on a sample with a relative concentration of 7:1 nanoparticle:DNA. The characteristic absorbances (indicated by the labels on the top spectrum) of the λ-DNA at 262 nm and of the gold nanoparticles at 520 nm were observed to decrease in concordance with each other.

for example, Figs 3 and 4, provide evidence for extended nanoassemblies formed from DNA and nanoparticles, which take the form of ribbons, bundles and branched ribbons. The image shown in Fig. 3 (inset) illustrates a typical ribbon/bundle structure. Portions of these structures consist of parallel λ-DNA scaffolds that are bound together by the polyvalent cationic nanoparticles as demonstrated in Fig. 3a,b and illustrated in the inset. In these portions the assemblies do not cross one another and the spacing between nanoparticles bound on adjacent chains is larger than the interparticle spacing (about 1.5 nm) along individual chains. The expected separation between nanoparticles on parallel assemblies in such a structure ranges from 1.5–3.5 nm, depending on the binding position of the nanoparticles on each scaffold. Other areas of the image provide evidence that some chains are assembled into 3D bundles: chains appear to cross one another, and, in some cases, the nanoparticles appear larger because two layers of them are overlapping.

Branching is an unexpected feature of the ribbon-like structures observed in this study (see Fig. 4). The observation of these previously unreported structures is important because it demonstrates the potential for forming complex, interconnected nanoparticle patterns on surfaces. The branched assembly shown in Fig. 4 is representative of those formed by using the conditions reported here. In each assembly observed, a branch point leading to two narrower ribbons disrupts the extended structure of a larger nanoparticle ribbon. The illustration in Fig. 4 (inset) provides one plausible explanation for the formation of the branched structures. The figure shows how the termination of a DNA strand at the interior of a ribbon might spawn two smaller ribbons on the other side of the branch. The fact that the combined widths of the daughter branches are approximately equal to the width of the parent ribbon is consistent with this hypothesis. The discovery of these branched structures supports the proposal that the use of deliberately branched DNA such as replication forks and Holliday junctions will be useful in templating molecularly interconnected arrays of nanoparticles through solution-phase assembly methods.

Although several approaches involving electrostatic assembly of cationic nanoparticles onto DNA have been reported to yield 2D and 3D structures[46,47], this study provides the first images in which the individual nanoparticles in the assembly can be visualized, showing the regular spacing of nanoparticles along the scaffolds and resolving the nanoparticles that cross-link the DNA scaffolds. Further control experiments confirm the role of the double-stranded DNA as a structural scaffold in the electrostatic assembly process. Mixtures of the thiocholine-stabilized nanoparticles and single-stranded DNA and mixtures of nanoparticles stabilized by anionic and neutral ligands with λ-DNA do not lead to extended, linear structures. In the former case, only small aggregates with short-range order were observed by TEM. In the latter two cases no evidence for interaction of the nanoparticles with the DNA scaffold was observed by either TEM or ultraviolet–visible spectroscopic analysis (see Supplementary Information). Thus, these data provide evidence that electrostatic assembly of thiocholine-stabilized nanoparticles onto double-stranded DNA in solution is a viable approach to preparing close-packed, templated 2D and 3D structures as well as linear nano particle assemblies.

Spectroscopic evidence further confirms binding of the functionalized gold nanoparticles to the DNA scaffolds, and also provides a method by which the assembly process in solution can be monitored. Because both building blocks (nanoparticles and DNA) have unique spectral signatures, we are able to monitor solution-phase assembly with visible spectroscopy (Fig. 5). As the solution phase assembly proceeds, the absorptions due to both building blocks decay simultaneously, which suggests that both components are being incorporated into an extended nanoassembly that precipitates over time. At long times (>30 minutes), an insoluble dark precipitate forms and little material remains in solution. These results suggest that cross-

linking of individual DNA scaffolds by the polyvalent gold nanoparticles leads to the formation of the dark solid. This hypothesis is further strengthened by the fact that, in the presence of $MgCl_2$ (saturated aqueous solution), aggregates are not formed. There is no evidence for interaction of the nanoparticle and DNA observable by ultraviolet–visible spectroscopy, and no extended structures are observed by TEM (see Supplementary Information).

A second set of ultraviolet–visible spectroscopy experiments confirms that the precipitate is an extended nanoassembly of DNA and nanoparticles and offers evidence that robust cross-linking holds the assemblies together. Neither heating to near 100 °C nor sonication for 10–15 min were effective in bringing the solid back into solution. However, on addition of KCN, which is known to cause the decomposition of gold nanoparticles[48], the dark solid rapidly re-disperses and the DNA absorbance at 262 nm reappears in the absence of the nanoparticle absorbance at 520 nm (see Supplementary Information). These results further suggest that the cross-linking of the DNA scaffolds by the nanoparticles leads to aggregation followed by precipitation.

Solution-phase assembly of interconnected nanoparticles onto DNA is a powerful approach to patterning 1D and 2D arrangements of nanoparticles for applications in nanoelectronics. The linear, ribbon-like and branched nanoparticle assemblies prepared by this method have a high degree of order and form close-packed, extended structures on surfaces that are readily observed by TEM. In addition, the assemblies appear to be thermally robust. Detailed analysis of the assembly structures suggests a possible mechanism for assembly that involves nucleation and growth. Higher-order structures composed of multiple nanoparticle/λ-DNA assemblies are also formed during the assembly process through cross-linking of the DNA scaffolds by the polyvalent nanoparticles. Branched assemblies are also observed and their unique structures are attributed to the termination of one of the internal DNA strands. Further investigation of the assembly mechanism will prove useful in the development of this method for nanostructure preparation. The attributes of this system (the accessibility of diverse structural types, close-packing of nanoparticles along the scaffolds, and the thermal stability of the assemblies) offer support for the idea that such assemblies should prove useful as building blocks in the construction of integrated nanoelectronic devices.

METHODS

SYNTHESIS OF CATIONICALLY FUNCTIONALIZED GOLD NANOPARTICLES

The nanoparticles used in this study were synthesized by using a procedure we developed that employs ligand exchange reactions between a small ($d_{core} < 2$ nm) phosphine-stabilized precursor nanoparticle and a water-soluble thiol ligand[31,32]. Briefly, the triphenylphosphine particles are synthesized by the $NaBH_4$ reduction of $HAuCl_4$ under phase-transfer conditions to generate the precursor nanoparticles that possess the requisite small core size and reactivity towards ligand exchange[32]. The water-soluble thiol ligand is synthesized according to the procedure outlined in the Supplementary Information. Water-soluble thiol-stabilized nanoparticles are synthesized from the precursor nanoparticles and the water-soluble ligand by a biphasic ligand-exchange reaction at room temperature[31]. The product nanoparticles possess the same small core size and narrow size dispersity as the precursor particles.

FORMATION OF NANOASSEMBLIES AND DEPOSITION ON SiO-COATED TRANSMISSION ELECTRON MICROSCOPY GRIDS FOR ANALYSIS

The nanoassemblies were formed by mixing the nanoparticles and the *Hind*III digest of λ-DNA (New England Biolabs, Beverly, Massachusetts, USA) in solution (each sample contained 0.35 μg μl^{-1} nanoparticles and 0.05 μg μl^{-1} λ-DNA in 110 μl of Ultrapure water (Barnstead, Boston, Massachusetts, USA)) and incubating at room temperature for a given period of time ranging from 5 min to 3 h. Samples were deposited by aerosoling approximately 10 μl of a premixed sample of λ-DNA and nanoparticles onto SiO-coated 400-mesh copper grids (Ted Pella, Redding, California, USA). Excess water was blotted off the grids with filter paper and then the samples were dried under ambient conditions before inspection by TEM. TEM was done on a Philips CM-12 microscope operating at an accelerating voltage of 120 kV. Images were recorded and processed as described previously[49].

SPECTROSCOPIC CHARACTERIZATION OF DNA/NANOPARTICLE ASSEMBLIES

UV-visible spectroscopy was performed on solutions of the same concentrations listed above. The KCN experiments were done by adding 0.5 ml of a 5 mM solution of KCN to a sample that had been incubated for approximately 3 h. A Hewlett-Packard HP8453 diode array ultraviolet–visible spectrometer was used, with a fixed slit width of 1 mm, and 1-cm quartz cuvettes.

Received 31 October 2002; accepted 11 January 2003; published 9 March 2003.

References

1. Tour, J. M. *et al.* Synthesis and preliminary testing of molecular wires and devices. *Chem. Eur. J.* **7,** 5118–5134 (2001).
2. Matsumoto, M., Tachibana, H. & Nakamura, T. Applications of organic conductors: molecular electronics. *Appl. Phys.* **4,** 759–790 (1994).
3. Sugi, M. Langmuir–Blodgett films – a course towards molecular electronics: a review. *J. Mol. Electron.* **1,** 3–17 (1985).
4. Luo, Y. *et al.* Two-dimensional molecular electronics circuits. *Chem. Phys. Chem.* **3,** 519–525 (2002).
5. Perkins, J. *et al.* Toward artificial molecular devices. *Mol. Electron. Bioelectron.* **12,** 69–74 (2001).
6. Heath, J. R. Nanoscale Materials. *Acc. Chem. Res.* **32,** 388 (1999).
7. Tans, S. J., Verschueren, A. R. M. & Dekker, C. Room-temperature transistor based on a single carbon nanotube. *Nature* **393,** 49–52 (1998).
8. Avouris, P., Collins, P. G. & Arnold, M. S. Engineering carbon nanotubes and nanotube circuits using electrical breakdown. *Science* **292,** 706–709 (2001).
9. Gardner, T. J., Frisbie, C. D. & Wrighton, M. S. Systems for orthogonal self-assembly of electroactive monolayers on Au and ITO: an approach to molecular electronics. *J. Am. Chem. Soc.* **117,** 6927–6933 (1995).
10. Vijayamohanan, K. & Aslam, M. Applications of self-assembled monolayers for biomolecular electronics. *Appl. Biochem. Biotech.* **96,** 25–39 (2001).
11. Fan, F.-R. F. *et al.* Determination of the molecular electrical properties of self-assembled monolayers of compounds of interest in molecular electronics. *J. Am. Chem. Soc.* **123,** 2454–2455 (2001).
12. Collier, C. P. *et al.* Electronically configurable molecular-based logic gates. *Science* **285,** 391–394 (1999).
13. Berven, C. A., Clarke, L., Mooster, J. L., Wybourne, M. N. & Hutchison, J. E. Defect-tolerant single-electron charging at room temperature in metal nanoparticle decorated biopolymers. *Adv. Mater.* **13,** 109–113 (2001).
14. Andres, R. P. *et al.* Self-assembly of a two-dimensional superlattice of molecularly linked metal clusters. *Science* **273,** 1690–1693 (1996).
15. Osifchin, R. G. *et al.* Synthesis of a quantum dot superlattice using molecularly linked metal clusters. *Superlattices Microstruct.* **18,** 283 (1995).
16. Kim, S. H. *et al.* Tunnel diodes fabricated from CdSe nanocrystal monolayers. *Appl. Phys. Lett.* **74,** 317–319 (1999).
17. Parthasarathy, R., Lin, X.-M. & Jaeger, H. M. Electron transport in metal nanocrystal arrays: the effect of structural disorder on scaling behavior. *Los Alamos Natl Lab., Prepr. Arch., Condens. Mat.* 1–4 (2001) (doi:arXiv:cond-mat/0102446).
18. Warner, M. G. & Hutchison, J. E. in *Synthesis, Functionalization, and Surface Treatment of Nanoparticles* (ed. Baraton, M.-I.) (American Scientific, San Francisco, 2002).
19. Wyrwa, D., Beyer, N. & Schmid, G. One-dimensional arrangements of metal nanoclusters. *Nano. Lett.* **2,** 410 (2002).
20. Clarke, L., Wybourne, M. N., Yan, M., Cai, S. X. & Keana, J. F. W. Transport in gold cluster structures defined by electron-beam lithography. *Appl. Phys. Lett.* **71,** 617–619 (1997).
21. Clarke, L. *et al.* Fabrication and near-room temperature transport of patterned gold cluster structures. *J. Vac. Sci. Technol. B* **15,** 2925–2929 (1997).
22. Hutchison, J. E. Nanoscience turns green. *Chem. Eng. News* **79,** 200 (2001).
23. Mirkin, C. A., Letsinger, R. L., Mucic, R. C. & Storhoff, J. J. A DNA-based method for rationally assembling nanoparticles into macroscopic materials. *Nature* **382,** 607–609 (1996).
24. Storhoff, J. J. & Mirkin, C. A. Programmed materials synthesis with DNA. *Chem. Rev.* **99,** 1849–1862 (1999).
25. Mirkin, C. A. Programming the assembly of 2 and 3D architectures with DNA and nanoscale inorganic building blocks. *Inorg. Chem.* **39,** 2258–2272 (2000).
26. McIntosh, C. M. *et al.* Inhibition of DNA transcription using cationic mixed monolayer protected gold clusters. *J. Am. Chem. Soc.* **123,** 7626–7629 (2001).
27. Sandhu, K. K., McIntosh, C. M., Simard, J. M., Smith, S. W. & Rotello, V. M. Gold nanoparticle-mediated transfection of mammalian cells. *Bioconjugate Chem.* **13,** 3–6 (2002).
28. Yonezawa, T., Onoue, S.-Y. & Kunitake, T. Formation of one-dimensional arrays of gold nanoparticles with DNA. *Kobunshi Ronbunshu* **56,** 855–859 (1999).
29. Yonezawa, T., Onoue, S.-Y. & Kunitake, T. Three-dimensional assembly of cationic gold nanoparticles and anionic organic components: DNA and a bilayer membrane. *Stud. Surf. Sci. Catal.* **132,** 623–626 (2001).
30. Torimoto, T. *et al.* Fabrication of CdS nanoparticle chains along DNA double strands. *J. Phys. Chem. B* **103,** 7799–8803 (1999).
31. Warner, M. G., Reed, S. M. & Hutchison, J. E. Small, water-soluble, ligand-stabilized gold nanoparticles synthesized by interfacial ligand exchange reactions. *Chem. Mater.* **12,** 3316–3320 (2000).
32. Weare, W. W., Reed, S. M., Warner, M. G. & Hutchison, J. E. Improved synthesis of small ($d_{CORE} \approx 1.5$ nm) phosphine-stabilized gold nanoparticles. *J. Am. Chem. Soc.* **122,** 12890–12891 (2000).
33. Brown, L. O. & Hutchison, J. E. Convenient preparation of stable, narrow-dispersity, gold nanocrystals by ligand exchange reactions. *J. Am. Chem. Soc.* **119,** 12384–12385 (1997).
34. Hagerman, P. J. Flexibility of DNA. *Annu. Rev. Biophys. Biomol. Struc.* **17,** 265–286 (1988).
35. Rivetti, C., Guthold, M. & Bustamante, C. Scanning force microscopy of DNA deposited onto mica: Equilibration versus kinetic trapping studied by statistical polymer chain analysis. *J. Mol. Biol.* **264,** 919–932 (1996).
36. Rivetti, C., Walker, C. & Bustamante, C. Polymer chain statistics and conformational analysis of DNA molecules with bends or sections of different flexibility. *J. Mol. Biol.* **280,** 41–59 (1998).
37. Sivolob, A. & Khrapunov, S. N. Electrostatic contribution to the bending of DNA. *Biophys. Chem.* **67,** 85–96 (1997).
38. Olins, D. E., Olins, A. L. & von Hippel, P. H. Model nucleoprotein complexes: Studies on the interaction of cationic homopolypeptides with DNA. *J. Mol. Biol.* **24,** 157–176 (1967).
39. Lees, C. W. & von Hippel, P. H. Hydrogen-exchange studies of deoxyribonucleic acid-protein complexes. Development of a filtration method and application to the deoxyribonucleic acid-polylysine system. *Biochemistry* **7,** 2480–2488 (1968).

40. Matthew, J. B. & Richards, F. M. Differential electrostatic stabilization of A-, B-, and Z-forms of DNA. *Biopolymers* **23,** 2743–2759 (1984).
41. McGhee, J. D. & Von Hippel, P. H. Theoretical aspects of DNA-protein interactions. Cooperative and noncooperative binding of large ligands to a one-dimensional homogeneous lattice. *J. Mol. Biol.* **86,** 469–89 (1974).
42. Leng, M. & Felsenfeld, G. The preferential interactions of polylysine and polyarginine with specific base sequences in DNA. *Proc. Natl Acad. Sci.* **56,** 1325–1332 (1966).
43. Olins, D. E., Olins, A. L. & von Hippel, P. H. On the structure and stability of DNA-protamine and DNA-polypeptide complexes. *J. Mol. Biol.* **33,** 265–281 (1968).
44. Rouzina, I. & Bloomfield, V. A. Competitive electrostatic binding of charged ligands to polyelectrolytes: Planar and cylindrical geometries. *J. Phys. Chem.* **100,** 4292–4304 (1996).
45. Rouzina, I. & Bloomfield, V. A. Competitive electrostatic binding of charged ligands to polyelectrolytes: practical approach using the non-linear Poisson-Boltzmann equation. *Biophys. Chem.* **64,** 139–155 (1997).
46. Kumar, A. *et al.* Linear superclusters of colloidal gold particles by electrostatic assembly on DNA templates. *Adv. Mater.* **13,** 341–344 (2001).
47. Sastry, M., Kumar, A., Datar, S., Dharmadhikari, C. V. & Ganesh, K. N. DNA-mediated electrostatic assembly of gold nanoparticles into linear arrays by a simple drop-coating procedure. *Appl. Phys. Lett.* **78,** 2943–2945 (2001).
48. Weisbecker, C. S., Merritt, M. V. & Whitesides, G. M. Molecular self-assembly of aliphatic thiols on gold colloids. *Langmuir* **12,** 3763–3772 (1996).
49. Brown, L. O. & Hutchison, J. E. Formation and electron diffraction studies of ordered 2-D and 3-D superlattices of amine stabilized gold nanocrystals. *J. Phys. Chem. B* **105,** 8911–8916 (2001).

Acknowledgements

The authors acknowledge Peter H. von Hippel for discussions and Ryan C. Chiechi for his assistance in the generation of Fig. 1. This work was supported by the National Science Foundation, the Camille and Henry Dreyfus Foundation (J.E.H. is a Camille and Henry Dreyfus Teacher Scholar) and the Department of Education GAANN program.
Correspondence should be addressed to J.E.H.
Supplementary Information is available on the website for *Nature Materials* (http://www.nature.com/naturematerials)

Competing financial interests

The authors declare that they have no competing financial interests.